applied sciences

MDPI

Article

Sargassum siliquastrum Aqueous Extract Attenuates Inflammation in RAW 264.7 Macrophages and Modulates Neuroinflammation in D-Galactose-Induced Aging Mice

Sung-Min Kim [1,2,†], Eun-Jung Park [2,3,†], Hae-Sun Park [3], Jihee Choi [2,3] and Hae-Jeung Lee [1,2,3,4,5,*]

[1] Department of Food Science and Biotechnology, Gachon University, Seongnam 13120, Republic of Korea; kimsm127@gachon.ac.kr
[2] Institute for Aging and Clinical Nutrition Research, Gachon University, Seongnam 13120, Republic of Korea; ejpark@gachon.ac.kr (E.-J.P.); jiheechoi@gachon.ac.kr (J.C.)
[3] Department of Food and Nutrition, Gachon University, Seongnam 13120, Republic of Korea; phs0130@gachon.ac.kr
[4] Department of Health Sciences and Technology, GAIHST, Gachon University, Incheon 21999, Republic of Korea
[5] Gachon Biomedical Convergence Institute, Gachon University Gil Medical Center, Incheon 21565, Republic of Korea
* Correspondence: skysea@gachon.ac.kr or skysea1010@gmail.com
† These authors contributed equally to this work.

Abstract

Inflammation and cellular senescence are fundamental contributors to aging and neurodegenerative disorders. Marine algae are increasingly acknowledged for their content of bioactive molecules capable of influencing inflammation and cellular aging. In this research, we examined the capacity of *Sargassum siliquastrum* aqueous extract (SSE) to counteract inflammatory responses in RAW 264.7 macrophages stimulated by lipopolysaccharide, as well as aging-related changes in a mouse model of D-galactose (D-gal)-induced aging. SSE treatment markedly lowered levels of pro-inflammatory cytokines, prostaglandin E_2, and nitric oxide. Furthermore, SSE attenuated the transcriptional activities of nuclear factor kappa-B (NF-κB) and activator protein 1, while modulating protein expression associated with NF-κB and mitogen-activated protein kinase (MAPK) signaling pathways in RAW 264.7 cells. In vivo, SSE reduced the phosphorylation levels of MAPKs in the hippocampus of D-gal-treated mice. Additionally, SSE modulated the expression of genes associated with cellular senescence and inflammation in the hippocampus and cerebral cortex. However, the apparent molecular effects were not accompanied by significant improvement in passive avoidance performance, which showed only a non-significant trend between the model control and SSE-administrated groups. Collectively, these findings suggest that SSE exerts anti-inflammatory effects in vitro and provide preliminary evidence of its potential to modulate D-gal-induced aging-related neuroinflammatory changes in mice.

Keywords: *Sargassum siliquastrum*; macroalgae; anti-inflammatory; neuroinflammation; NF-κB; MAPK

Check for updates

Academic Editor: Leonel Pereira

Received: 15 January 2026
Revised: 8 March 2026
Accepted: 11 March 2026
Published: 12 March 2026

Copyright: © 2026 by the authors. Licensee MDPI, Basel, Switzerland. This article is an open access article distributed under the terms and conditions of the Creative Commons Attribution (CC BY) license.

1. Introduction

The inflammatory response is a vital biological response that defends the host from harmful stimuli, including pathogens, abnormal cells, and chemical irritants. It is responsible for maintaining homeostasis and immunity [1]. Once tissues are damaged or invaded by pathogens, an acute inflammatory response is rapidly activated and generally relieved

within a few days. However, if the body fails to eliminate the cause of inflammation or is continuously exposed to irritants, uncontrolled acute inflammation may lead to chronic inflammation, which is less intense but persistent [2]. Importantly, age-related chronic inflammation may increase oxidative stress and promote microglial and astrocyte priming, processes implicated in inflammaging and age-related cognitive decline [3]. Additionally, chronic inflammatory responses typically involve prolonged activation within immune cell populations and the increased generation of inflammatory molecules such as nitric oxide (NO), tumor necrosis factor-alpha (TNF-α), and interleukin-1 beta (IL-1β) [4]. Systemically produced pro-inflammatory cytokines can affect central inflammatory responses through multiple mechanisms, including active transport across the blood–brain barrier and activation of circumventricular organs, potentially contributing to neuroinflammation and cognitive impairment [3]. Therefore, modulation of systemic inflammatory signaling may influence inflammatory status in the brain and be associated with aging-related neuroinflammatory changes. Several natural products and bioactive compounds have been reported to reduce inflammatory markers in both systemic circulation and brain tissue [5,6]. These findings support the concept that modulation of excessive and chronic inflammatory responses may contribute to the prevention or attenuation of immune disorders and age-related neuroinflammatory changes.

Macrophages function as central components of innate immunity, eliminating pathogens through phagocytosis while drawing additional immune cells to areas where damage or infection has occurred [7]. RAW 264.7 macrophages are employed to investigate potential anti-inflammatory properties of natural products derived from various sources, including marine algae, plants, and microorganisms. Lipopolysaccharide (LPS) is frequently utilized to activate RAW 264.7 macrophages, which are then triggered to generate inflammatory mediators like NO and various pro-inflammatory cytokines [8–10]. Core signal transduction pathways, such as nuclear factor kappa-B (NF-κB) and mitogen-activated protein kinases (MAPKs), are pivotal in inflammatory responses by controlling the transcription of inflammatory genes and mediating cellular responses to extracellular stimuli [11]. As dysregulation and overexpression of these pathways contribute to prolonged inflammation and various diseases, modulating their activity is a strategic approach to attenuate excessive inflammation.

Seaweeds (also known as marine macroalgae), traditionally consumed as food, are abundant in nutrients and bioactive substances, including polysaccharides, proteins, polyphenols, minerals, and vitamins, which highlight their potential as functional food sources [12]. Approximately 11,000 species of seaweed are known worldwide and are generally classified as brown, red, or green algae [13,14]. *Sargassum* (*S.*), a type of brown alga, has long served as both a food source and a traditional medicine throughout East Asian countries. It is one of eight genera that dominate maricultured seaweeds worldwide [15,16]. Recently, various beneficial bioactive effects of *Sargassum* spp. have been reported. In particular, *S. confusum* exhibited inflammation-modulating effects in RAW 264.7 macrophages challenged with LPS, and alleviated ear edema in mouse models [17]. Meanwhile, *S. horneri* inhibited lipid formation and accumulation in mice receiving a high-fat diet as well as in differentiated 3T3-L1 adipocytes [18]. *S. fusiforme* has been reported to alleviate hepatotoxicity and nephrotoxicity in cisplatin-induced mice [19]. *S. siliquastrum* is one of six seaweeds (*S. siliquastrum*, *S. horneri*, *S. serratifolium*, *S. sagamianum*, *S. confusum*, and *S. thunbergii*) authorized as novel food ingredients by the Korean Ministry of Food and Drug Safety in 2016; it has been reported to contain several bioactive compounds, including meroterpenoids of the chromene class and polyunsaturated fatty acids [20,21]. A previous study reported the anti-inflammatory effects of *S. siliquastrum* ethanol extract in LPS-stimulated RAW 264.7 cells [21]. However, to the best of our knowledge, the anti-inflammatory effects

of the aqueous extract have not been evaluated, and the potential neuroprotective effects of *S. siliquastrum* extracts have not been investigated in vivo. In the present study, we selected the aqueous extract because it is more directly applicable to dietary and functional food development and avoids potential issues associated with organic solvent residues. We examined the anti-inflammatory properties of *S. siliquastrum* aqueous extract (SSE) using RAW 264.7 cells and conducted a preliminary in vivo evaluation to determine its potential effects on D-galactose (D-gal)-induced aging-related neuroinflammatory changes in the mouse brain.

2. Materials and Methods

2.1. Procedure for Preparing S. siliquastrum Extract

SSE was provided by Seoho Lab Co., Ltd. (Bucheon, Republic of Korea). It was prepared following standard procedures. Briefly, the raw material was obtained from the vicinity of Jeju Island in South Korea, rinsed, air-dried, and ground. Samples were extracted in distilled water at a 1:20 (*w*/*w*) ratio and heated for 2 h at temperatures ranging from 90 to 95 °C. After the extraction step, the mixtures were passed through Whatman No. 2 filter paper to eliminate insoluble residues, and the resulting filtrates were concentrated under reduced pressure to obtain hot-water extracts. The extract was stored at −20 °C until further use and dissolved in deionized water for subsequent experiments. The extraction yield was approximately 12.88%. The total phenolic content was determined using the Folin–Ciocalteu method with slight modifications and expressed as gallic acid equivalents (GAE) [22]. The analysis was conducted by the Korea Health Functional Food Institute (KHFF), an accredited organization recognized by the Korea Laboratory Accreditation Scheme. Briefly, 1 mL of diluted SSE was mixed with 5 mL of 10% Folin–Ciocalteu reagent at room temperature. After 3 min, 4 mL of 7.5% Na_2CO_3 solution was added, and the mixture was incubated for 1 h in the dark. The absorbance was measured at 765 nm using a UV/Vis spectrophotometer (Agilent Technologies, Santa Clara, CA, USA). The total phenolic content was 32.52 mg GAE/g SSE.

2.2. High-Performance Liquid Chromatography (HPLC)

Mannitol content in SSE was analyzed at KHFF using an HPLC system (Agilent Technologies, Santa Clara, CA, USA) equipped with an evaporative light scattering detector and a carbohydrate high-performance column (4.0 µm, 4.6 × 250 mm; Waters, Milford, MA, USA). The mobile phase consisted of acetonitrile and water (81.5:18.5, *v*/*v*). The flow rate was 1.2 mL/min, the injection volume was 3 µL, and the total run time was 30 min. The column temperature was maintained at 40 °C. A standard stock solution was prepared by dissolving mannitol (purity ≥ 99%; Sigma-Aldrich, St. Louis, MO, USA) in deionized water. Mannitol content was determined to be 62.62 mg/g.

2.3. Cell Culture and Viability Assay

The RAW 264.7 macrophage cell line was obtained from the American Type Culture Collection (Manassas, VA, USA). Cells were maintained in a 5% CO_2 incubator at 37 °C in Dulbecco's modified Eagle medium (Corning, Corning, NY, USA) supplemented with 10% fetal bovine serum and 1% antibiotic–antimycotic solution (Gibco, Grand Island, NY, USA). Cells were subcultured before reaching 80% confluence to maintain optimal growth. To evaluate the effects of SSE on viability, the Cell Counting Kit-8 (CCK-8) assay (Dojindo Laboratories, Kumamoto, Japan) was performed. Briefly, cells were exposed to SSE (25–100 µg/mL) for 24 h under conditions either without or with 1 µg/mL LPS. Subsequently, the culture medium was substituted with fresh medium supplemented with 10% CCK-8. After incubating for 1 h, the absorbance was assessed at 450 nm using

a microplate reader (BioTek Instruments, Inc., Winooski, VT, USA). To assess potential endotoxin contamination, polymyxin B (10 μg/mL; Sigma-Aldrich, St. Louis, MO, USA) was added to the working treatment medium and incubated for 30 min prior to treatment. After 24 h of treatment, cell viability was assessed using the CCK-8 assay. Cytotoxicity was evaluated using the CytoTox 96® Non-Radioactive Cytotoxicity Assay (Promega, Madison, WI, USA) according to the manufacturer's instructions.

2.4. NO, PGE_2, and Pro-Inflammatory Cytokine Measurements

Cells were co-treated with 1 μg/mL LPS and SSE for 24 h, and the culture medium was then harvested from each well. To remove debris, the collected culture medium was centrifuged at 3000× *g* for 5 min at 4 °C, and used to determine NO production and the concentrations of PGE_2 and three pro-inflammatory cytokines (TNF-α, IL-1β, and interleukin-6 (IL-6)). NO production was measured as nitrite using the Griess Reagent System (Promega, Madison, WI, USA), while the concentrations of PGE_2, TNF-α, IL-1β, and IL-6 were determined using commercial enzyme-linked immunosorbent assay kits (R&D Systems, Minneapolis, MN, USA) according to the manufacturer's instructions.

2.5. Luciferase Assay

Cells were transfected using FuGENE® HD Transfection Reagent (Promega, Madison, WI, USA). Briefly, 24 h after seeding the cells into 96-well white plates, the cells were transfected with the pNL1.1.TK vector (Promega, Madison, WI, USA) together with either the 3 × κB [23] or 3 × AP1pGL3 (Addgene, Watertown, MA, USA) [24] luciferase reporter plasmid. The 3 × AP1pGL3 (3 × AP-1 in pGL3-basic) was a gift from Alexander Dent (Addgene plasmid #40342; http://n2t.net/addgene:40342 (accessed on 10 March 2026); RRID: Addgene_40342). pNL1.1.TK was used as an internal control to normalize for transfection efficiency. Cells were subsequently exposed to 1 μg/mL LPS together with varying doses of SSE for a duration of 24 h. Dual luciferase signals were quantified with a luciferase-based detection system (Promega, Madison, WI, USA) using a microplate luminometer (Promega, Madison, WI, USA). The 3 × κB- and 3 × AP1-Luc activities were normalized to NanoLuc signals.

2.6. Western Blotting

RAW 264.7 cells were co-treated with LPS and SSE for 15 min to assess NF-κB inhibitor alpha (IκBα); 30 min to assess p38, c-Jun N-terminal kinase (JNK), and extracellular signal-regulated kinase (ERK)1/2; and 60 min to assess NF-κB. For in vivo analysis, hippocampal tissues were homogenized and incubated on ice for 30 min, followed by centrifugation at 10,000× *g* for 5 min at 4 °C to obtain the clear supernatant. The subsequent procedures were performed as described in our previous study [25].

2.7. Quantitative Reverse Transcription Polymerase Chain Reaction (qRT-PCR)

Total RNA was isolated from RAW 264.7 cells co-treated with LPS and SSE for 24 h using a commercial extraction kit (iNtRON Biotechnology, Seongnam, Republic of Korea). For the in vivo experiments, total RNA was also isolated from mouse hippocampal and cerebral cortex tissues. Subsequent experimental procedures were conducted as described in our previous study [25]. Gene expression was quantified using β-actin as a reference gene, and primer sequences are provided in Table 1.

Table 1. List of primer sequences for qRT-PCR.

Genes	Accession Number	Primer Sequence (5′–3′)
iNOS	NM_010927.4	TTCCAGAATCCCTGGACAAG TGGTCAAACTCTTGGGGTTC
COX-2	NM_011198.5	AGAAGGAAATGGCTGCAGAA GCTCGGCTTCCAGTATTGAG
TERT	NM_009354.2	F: ACTCCGTTGTCATCGAGCAG R: TGCGTATAGCACCTGTCACC
p53	NM_011640.4	F: GCATGAACCGCCGACCTATCC R: CCCAGGGCAGGCACAAACAC
p21	NM_001111099.2	F: GTGAGGAGGAGCATGAATGGA R: GCACCTTTTATTCTGCTGGCAA
p16	NM_001040654.1	F: GTGTGCATGACGTGCGG R: CACCTGAATCGGGGTACGAC
NF-κB1 (p105)	NM_008689.3	F: CAGGATGAGAATGGGGACAG R: CAAGTGCAGAGGTGTCTGAT
RelA (p65)	NM_009045.5	F: CCATTGTGTTCCGGACTCCT R: GGTGGCGATCATCTGTGTCT
TNF-α	NM_013693.3	F: AGGCGGTGCCTATGTCTCAG R: GCCATTTGGGAACTTCTCATCCC
IL-1β	NM_008361.4	F: GTGGCAGCTACCTGTGTCTT R: AATGGGAACGTCACACACCA
IL-6	NM_001314054.1	F: AGTTGCCTTCTTGGGACTGA R: CAGAATTGCCATTGCACAAC
β-actin	NM_007393.5	F: CCACAGCTGAGAGGGAAATC R: AAGGAAGGCTGGAAAAGAGC

2.8. Animal Procedures

Male ICR mice (8 weeks old) were obtained from Daehan Biolink Co. (Eumseong, Republic of Korea). Following a 7-day acclimation period, the animals were maintained under standardized environmental settings (temperature 20–25 °C; humidity 50–55%; light-dark cycle 12 h/12 h) with unrestricted access to rodent chow and drinking water. A total of ten mice were randomly assigned to either the model control (MC) group or the SSE-administered groups using a random number generator. D-gal injection (500 mg/kg/day) was initiated prior to and maintained throughout the SSE administration period to reflect the gradual and continuous development of aging conditions. This experimental schedule was designed to evaluate the modulatory effects of SSE under conditions of ongoing D-gal-induced aging rather than to exclusively assess preventive or restorative effects [26–28]. Additionally, it has been reported that a dosage of 500 mg/kg of D-gal induces neuroinflammation and cognitive impairment in ICR mice [29,30]. All animals received intraperitoneal injections of D-gal (Sigma-Aldrich, St. Louis, MO, USA) for a duration of 8 weeks. From weeks 5 to 8, the MC and SSE groups were given oral sterile saline or 100 mg/kg/day of SSE, respectively. The SSE dose was selected based on previous studies of seaweed aqueous extracts demonstrating biological effects, including anti-inflammatory effects, without significant adverse effects [31–33]. Whole blood for serum collection and cerebral cortex tissue were harvested from each mouse after 12 h of fasting and sacrifice in a CO_2 chamber, and the collected samples were stored at −80 °C. No animals were excluded from the following experiments and analyses. All animal procedures were approved by the Institutional Animal Care and Use Committee (GU1-2024-IA0037) of Gachon University and were conducted in accordance with the ARRIVE guidelines.

2.9. Passive Avoidance Test

Testing was performed over two consecutive days using a step-through apparatus (Ugo Basile, Gemonio, Italy), equipped with illuminated and darkened chambers separated by a sliding guillotine gate. On the initial training day, individual mice were introduced into the illuminated compartment and permitted to move freely. Sixty seconds later, access to the dark compartment was provided. After complete entry into the dark side, the gate was closed, and the animal was returned to its home cage after 10 s. After being in the cage for 30 min, the same mouse was put back in the lit compartment, and the gate was lifted after 5 s. Upon re-entry into the dark chamber, the gate was immediately closed and an electric shock (0.5 mA for 3 s) was administered via the electrified bottom grid. The mouse was then placed back in its cage for 2 min, and the same procedure was repeated. The training session was terminated when the mouse remained immobile in the light chamber for at least 2 min. On the second day of step-through latency measurement, latency was evaluated by placing the mouse in the illuminated compartment and recording the duration required to completely cross into the dark chamber after opening the gate. Animals that did not enter within 300 s were assigned a latency of 300 s. Although the investigator was aware of group allocation during the experiment, behavioral testing and outcome assessments were monitored by an independent researcher not directly involved in the study to minimize potential bias.

2.10. Statistical Analysis

All data are expressed as the mean ± SD of at least three independent experiments. Statistical analyses were performed using GraphPad Prism 10 software (GraphPad Software, San Diego, CA, USA). Normality was assessed using the Shapiro–Wilk test. For multiple comparisons, Welch's ANOVA followed by the Dunnett's T3 test was used. For data analyzed by two-way ANOVA, Dunnett's test was used for comparisons with the vehicle control, whereas Šídák's test was used for pairwise comparison. Comparisons between two groups were performed using an unpaired *t*-test with Welch's correction. A p value < 0.05 was considered statistically significant.

3. Results

3.1. SSE Attenuates LPS-Induced Increases in Cell Viability in RAW 264.7 Macrophages

Viability assays were performed to determine appropriate SSE concentrations and to investigate the effects of SSE on LPS-induced RAW 264.7 cells. As shown in Figure 1a, SSE showed no cytotoxicity up to 100 μg/mL after 24 h of treatment. Cell viability did not differ between SSE-treated cells in the absence or presence of polymyxin B, suggesting that the observed effects were not attributable to endotoxin contamination. LPS treatment notably increased cell viability, whereas co-treatment with 50 and 100 μg/mL SSE attenuated this increase (Figure 1b). Importantly, cytotoxicity assay results indicated that SSE did not induce cytotoxicity in LPS-stimulated cells at these concentrations (Figure 1c). Accordingly, these SSE treatment concentrations were applied in all subsequent experiments.

3.2. SSE Suppresses NO and PGE_2 Levels Through the Regulation of Their Associated mRNA Expression

We next measured NO and PGE_2 levels in the culture medium, along with the mRNA expression levels of inducible nitric oxide synthase (iNOS) and cyclooxygenase-2 (COX-2). As illustrated in Figure 2a, LPS exposure led to a significant elevation in NO production, whereas co-treatment with SSE resulted in a notable reduction. Consistently, the mRNA expression of iNOS, which is responsible for regulating NO production, was also upregulated by LPS, but was downregulated by SSE. Additionally, the production of the key mediator

PGE_2 was markedly increased by LPS (Figure 2b). SSE inhibited both PGE_2 production and the mRNA expression of its regulatory gene, COX-2.

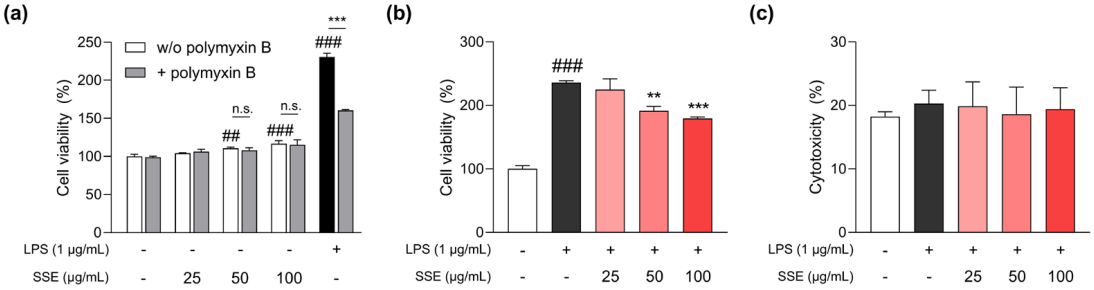


Figure 1. Effects of SSE on viability and cytotoxicity in RAW 264.7 cells. (**a**) Viability of cells treated with 25, 50, and 100 μg/mL of SSE in the absence or presence of polymyxin B for 24 h (n = 3). (**b**) Viability in cells treated with the same concentrations of SSE and 1 μg/mL LPS for 24 h (n = 3). (**c**) Cytotoxicity in cells treated with 25–100 μg/mL of SSE and 1 μg/mL LPS for 24 h (n = 3). Data are presented as mean ± SD. Welch's ANOVA followed by the Dunnett's T3 test, and two-way ANOVA followed by Dunnett's multiple comparisons test or Šídák's multiple comparisons test were used for statistical analysis. ## $p < 0.01$, ### $p < 0.001$ vs. vehicle control; ** $p < 0.01$, *** $p < 0.001$ vs. LPS-only group; n.s., not significant.

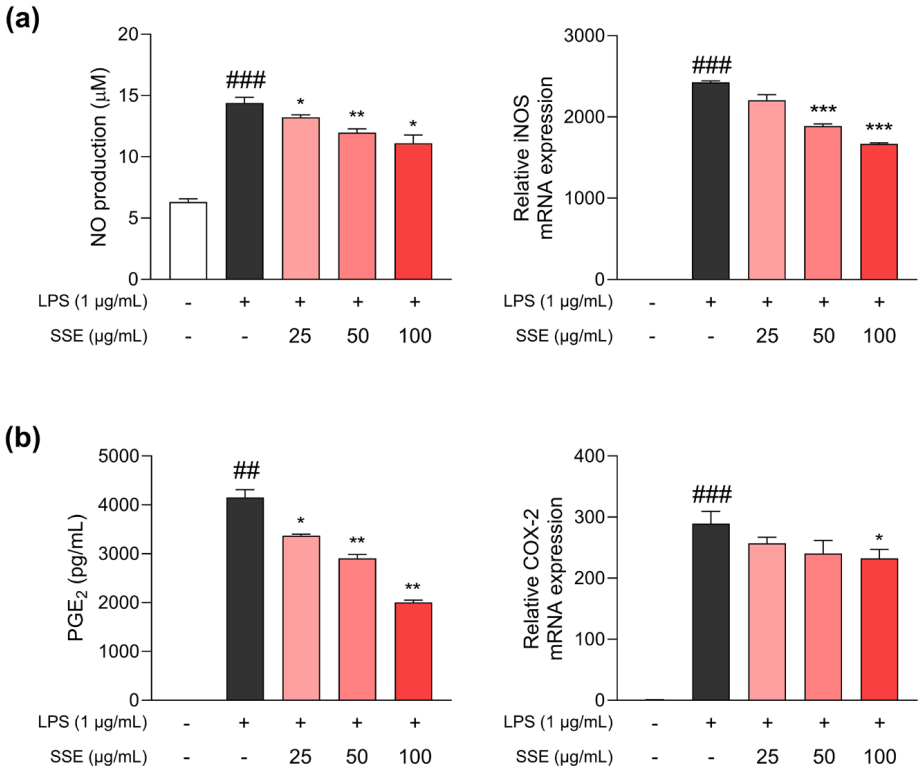


Figure 2. SSE alters NO and PGE_2 production, as well as iNOS and COX-2 mRNA expression, in RAW 264.7 cells co-treated with LPS for 24 h. (**a**) NO production and iNOS mRNA expression levels (n = 3); (**b**) PGE_2 concentration and COX-2 mRNA expression levels (n = 3). The iNOS and COX-2 expression levels were normalized to those of β-actin. Data are presented as mean ± SD. Welch's ANOVA followed by the Dunnett's T3 test was used for statistical analysis. ## $p < 0.01$, ### $p < 0.001$ vs. vehicle control; * $p < 0.05$, ** $p < 0.01$, *** $p < 0.001$ vs. LPS-only group.

3.3. SSE Inhibits Pro-Inflammatory Cytokine Production

We further investigated whether SSE attenuates the production of pro-inflammatory cytokines, TNF-α, IL-6, and IL-1β, predominantly secreted from activated macrophages. As shown in Figure 3, their concentrations in RAW 264.7 culture medium were markedly

increased by LPS stimulation. In contrast, treatment with SSE significantly decreased the concentrations of these cytokines. Collectively, these results support the hypothesis that SSE exhibits anti-inflammatory effects.

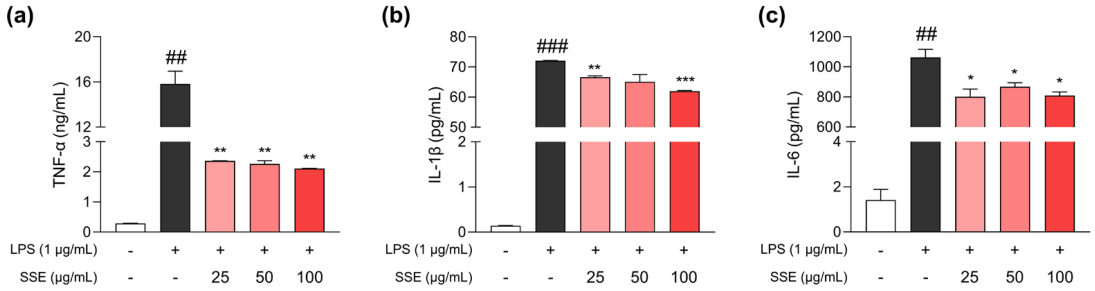


Figure 3. SSE decreases the production of pro-inflammatory cytokines TNF-α, IL-1β, and IL-6 in RAW 264.7 cells. (**a**) TNF-α, (**b**) IL-1β, and (**c**) IL-6 concentrations in cells co-treated with SSE and 1 μg/mL LPS for 24 h (n = 3). Data are presented as mean ± SD. Welch's ANOVA followed by the Dunnett's T3 test was used for statistical analysis. ## $p < 0.01$, ### $p < 0.001$ vs. vehicle control; * $p < 0.05$, ** $p < 0.01$, *** $p < 0.001$ vs. LPS-only group.

3.4. SSE Modulates NF-κB and MAPK Signaling

As SSE exhibits anti-inflammatory effects, we examined its impact on the NF-κB and MAPK pathways. Exposure to LPS significantly enhanced NF-κB-dependent luciferase activity in transiently transfected macrophages, while SSE markedly reduced this activity (Figure 4a). Moreover, LPS-induced phosphorylation levels of IκBα and NF-κB were reduced upon SSE treatment (Figure 4b). Total IκBα levels were increased by SSE treatment, indicating inhibition of IκBα degradation. We further assessed the impact of SSE on activator protein 1 (AP-1), which plays a central role in inflammatory responses. As shown in Figure 5a, AP-1 activity was elevated by LPS, whereas SSE decreased it. As AP-1 signaling is known to be regulated by upstream MAPKs, we examined the influence of SSE on MAPK signaling. Phosphorylation levels of p38, JNK, and ERK1/2 were significantly decreased by SSE (Figure 5b).

3.5. SSE Attenuates Senescence- and Inflammation-Associated Gene Expression in D-Gal-Induced Mouse Brain

We hypothesized that SSE would exert beneficial effects on D-gal-induced alterations in the mouse brain, as several natural products and bioactive compounds with anti-inflammatory properties have been reported to influence aging-related processes. Body weight and food consumption did not differ significantly between the MC and SSE-administered groups (Figure 6a,b). As shown in Figure 6c, the step-through latency tended to be longer in the SSE-administered group relative to the MC group; however, this difference did not reach statistical significance (50.78 ± 37.57 s in the MC group; 131.00 ± 109.85 s in the SSE group; p = 0.184). At the molecular level, SSE administration upregulated the mRNA expression of telomerase reverse transcriptase (TERT) and downregulated the expression of p53, p21, and p16, which are associated with cellular senescence and cell cycle regulation, in the hippocampal and cerebral cortex tissues (Figure 7a,b). Moreover, the mRNA expression levels of NF-κB1, RelA, TNF-α, IL-1β, and IL-6 were markedly reduced in the SSE-administered group (Figure 7c,d). The phosphorylation levels of ERK1/2, JNK, and p38 were lower in the hippocampus of the SSE group compared with those of the MC group (Figure 8). Taken together, these findings suggest that SSE modulates aging-related and inflammatory molecular markers in the brain of D-gal-treated mice; however, its impact on behavioral outcomes remains to be clarified.

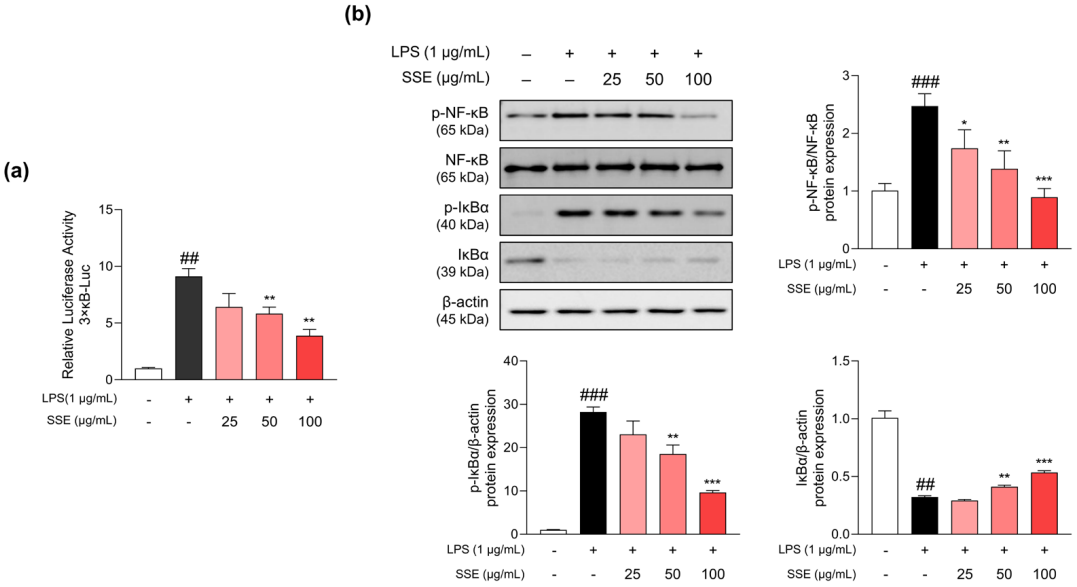


Figure 4. Effects of SSE on NF-κB transcriptional activity and protein expression of NF-κB and IκBα in RAW 264.7 cells. (**a**) Luciferase activity in cells transiently transfected with 3 × κB-Luc, followed by treatment with various concentrations of SSE and 1 μg/mL LPS for 24 h (n = 3). (**b**) Representative Western blot images of NF-κB and IκBα and quantification of their expression and phosphorylation (n = 3). Phosphorylated NF-κB was normalized to total NF-κB, while phosphorylated and total IκBα levels were normalized to β-actin. Data are presented as mean ± SD. Welch's ANOVA followed by the Dunnett's T3 test was used for statistical analysis. ## $p < 0.01$, ### $p < 0.001$ vs. vehicle control; * $p < 0.05$, ** $p < 0.01$, *** $p < 0.001$ vs. LPS-only group.

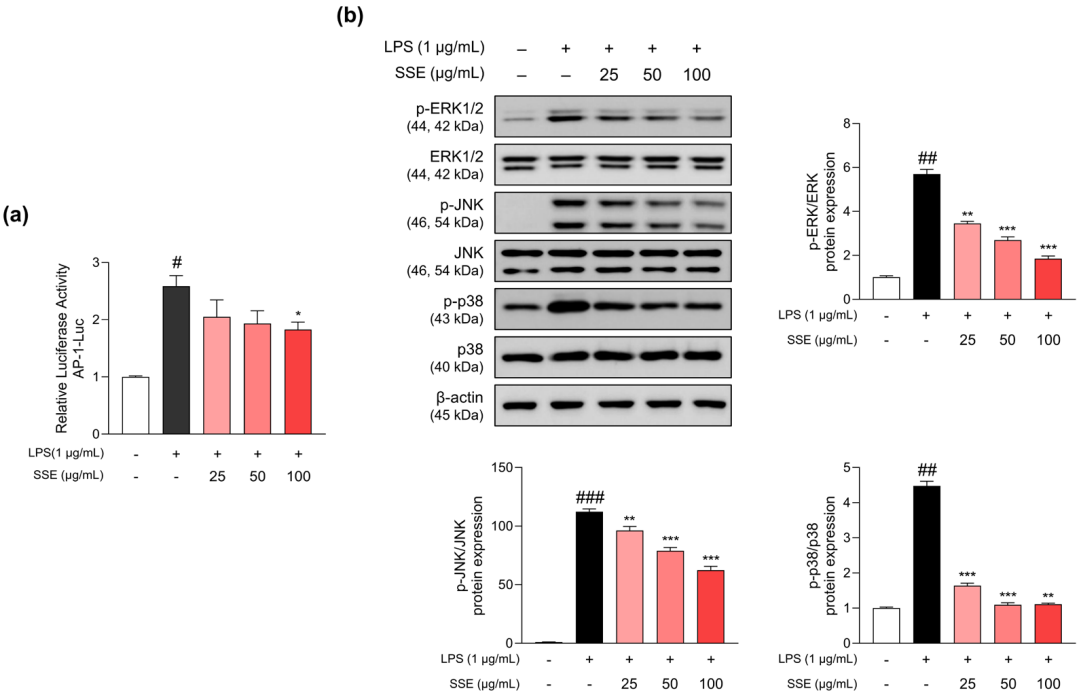


Figure 5. Effects of SSE on AP-1 transcriptional activity and MAPK protein expression in RAW 264.7 cells. (**a**) Luciferase activity in cells transiently transfected with 3 × AP1-Luc, followed by treatment with various concentrations of SSE and 1 μg/mL LPS for 24 h (n = 3). (**b**) Representative Western blot images of ERK1/2, JNK, and p38 and quantification of their expression (n = 3). The phosphorylation levels were normalized to their total protein levels. Data are presented as mean ± SD. Welch's ANOVA followed by the Dunnett's T3 test was used for statistical analysis. # $p < 0.05$, ## $p < 0.01$, ### $p < 0.001$ vs. vehicle control; * $p < 0.05$, ** $p < 0.01$, *** $p < 0.001$ vs. LPS-only group.

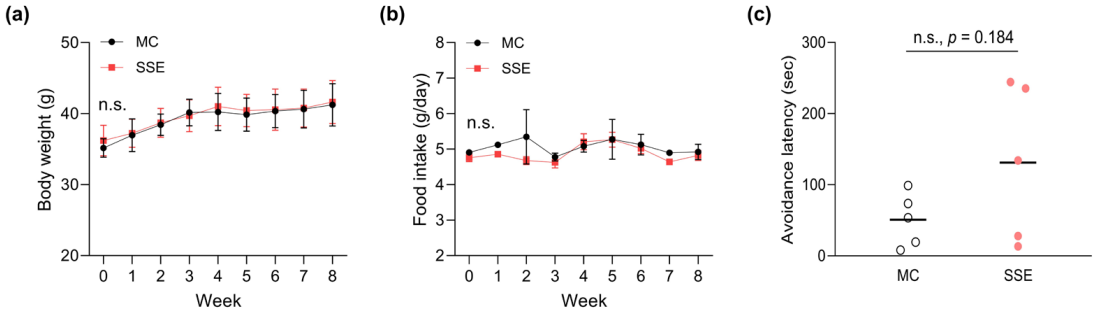


Figure 6. Effects of SSE on body weight, food intake, and avoidance latency in D-gal-induced aging mice. (**a**) Changes in body weight over time ($n = 5$/group). (**b**) Mean daily food intake over time ($n = 5$/group). (**c**) Avoidance latency measured 24 h after training ($n = 5$/group). Each dot represents an individual mouse. Body weight and food intake data are presented as mean ± SD. Two-way ANOVA followed by Šídák's multiple comparisons test and an unpaired *t*-test with Welch's correction were used for statistical analysis. MC, model control group; SSE, SSE-treated group; n.s., not significant.

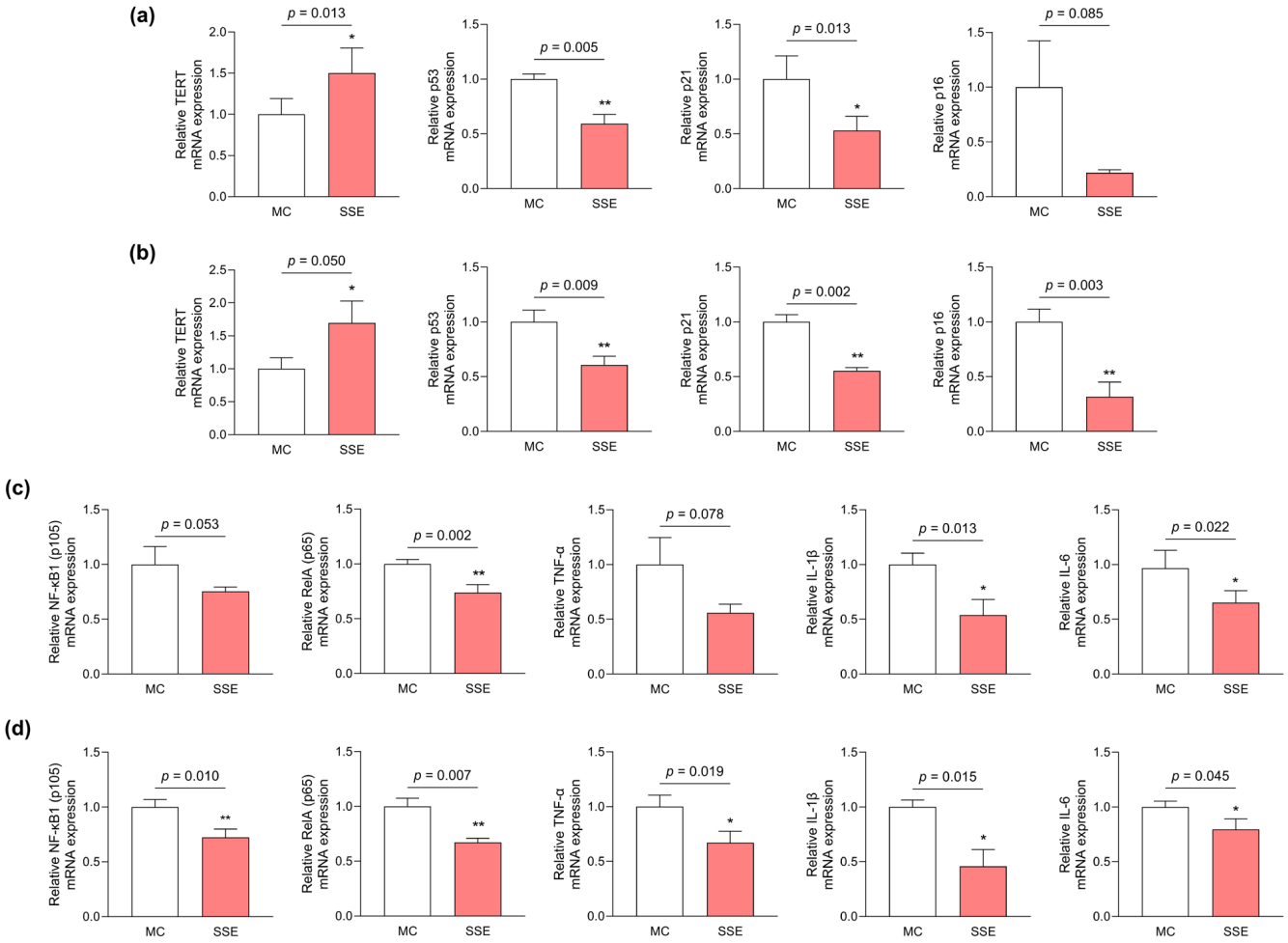


Figure 7. SSE reduces senescence- and inflammation-related gene expression in brains of D-gal-induced aging mice. (**a**,**b**) mRNA expression levels of TERT, p53, p21, and p16 in the cerebral cortex and hippocampal tissues, respectively ($n = 3$–4). (**c**,**d**) mRNA expression levels of NF-κB1, RelA, TNF-α, IL-1β, and IL-6 in the cerebral cortex and hippocampal tissues, respectively ($n = 3$–4). All levels were normalized to those of β-actin. Data are presented as mean ± SD. An unpaired *t*-test with Welch's correction was used for statistical analysis. * $p < 0.05$, ** $p < 0.01$ vs. MC. MC, model control group; SSE, SSE-treated group.

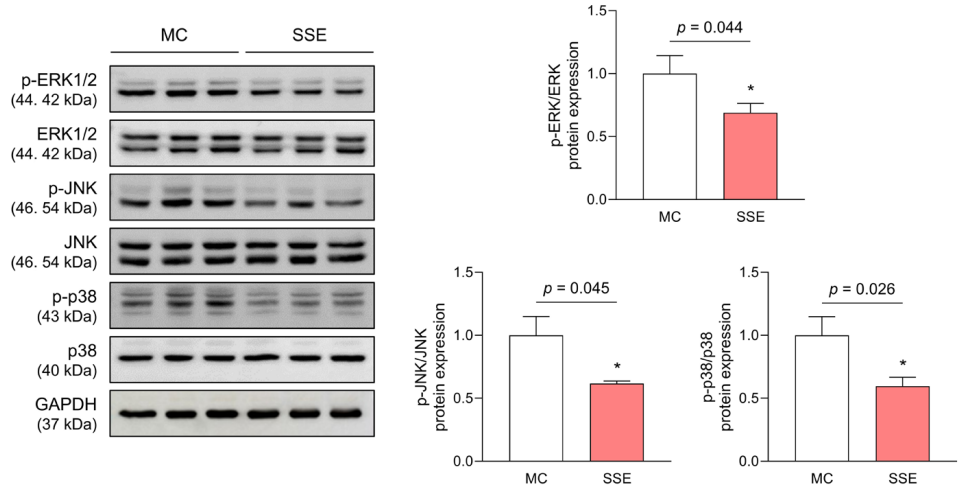


Figure 8. Effects of SSE on MAPK protein expression in the hippocampus of D-gal-treated mice. Representative Western blot images of ERK1/2, JNK, and p38 (**left** panel) and quantification of their levels (**right** panel) (n = 3). The phosphorylation levels were normalized to their total protein levels. Data are presented as mean ± SD. An unpaired t-test with Welch's correction was used for statistical analysis. * $p < 0.05$ vs. MC. MC, model control group; SSE, SSE-treated group.

4. Discussion

Severe or chronic inflammation is implicated in the pathogenesis of many diseases; therefore, diverse anti-inflammatory agents are helpful in regulating and alleviating unexpected inflammation. Numerous studies have demonstrated that natural products, including macroalgae, herbal medicines, and bioactive compounds, have potential as anti-inflammatory agents. Reshma et al. reported that agar derived from *Laminaria digitata* exhibits anti-aging properties in a D-gal-induced mouse model [34]. Ligustilide, one of the major bioactive components of *Angelica sinensis*, has been shown to suppress inflammation induced by LPS, as well as attenuating neurotoxicity in mice subjected to D-gal-induced aging [35,36]. These results suggest that various bioactive substances with anti-inflammatory effects may attenuate D-gal-induced aging by regulating inflammation.

S. siliquastrum has been reported to contain various meroterpenoids, including chromene-type compounds, as well as meroditerpenoids belonging to the nahocol, isonahocol, and sargahydroquinoic acid classes [37]. Sargachromanol G, sargachromanol E, and fucoxanthin derivatives, isolated from *S. siliquastrum*, have been reported to exhibit anti-inflammatory effects [38–40]. Qi et al. identified chromane-type meroterpenoids (sargasilols A–I) from *S. siliquastrum* and found that sargasilol A significantly inhibited inflammatory responses via the NF-κB signaling pathway in BV2 cells [41]. Sargasilols J–N were newly isolated in 2024; in 2025, 9′-deoxysargachromanol E and 3′,4′-dihydro-4′-hydroxysargachromanol I were isolated, which exhibited anti-neuroinflammatory effects [42,43]. Although these findings suggest that *S. siliquastrum* contains compounds with anti-inflammatory and anti-neuroinflammatory effects, the presence of the aforementioned compounds, including sargachromanols and sargasilols, in the present SSE was not confirmed in this study. Therefore, the observed anti-inflammatory effects of SSE cannot be directly linked to these compounds. We confirmed the presence of mannitol in the SSE and quantified its content. Given that mannitol has been reported to exhibit anti-inflammatory, antioxidant, and wound healing properties, it may partially contribute to the observed anti-inflammatory effects [44,45]. However, further chemical characterization will be required to better identify the bioactive compounds responsible for the anti-inflammatory and anti-neuroinflammatory effects of SSE. Furthermore, fractionation of SSE or isolation of individual compounds will be

necessary to determine whether the modulation of NF-κB and MAPK signaling can be attributed to specific bioactive compounds.

NO, PGE_2, and pro-inflammatory cytokines are key inflammatory mediators with multifaceted functions in physiological processes, such as host defense and immune regulation. As excessive production of these mediators by activated macrophages can lead to detrimental effects, their levels must be maintained within the physiological range to preserve immune balance. NO mediates immune cell signaling, pathogen elimination, and vascular homeostasis; however, under conditions of elevated NO and superoxide anion (O_2^-), such as infection, tissue injury, or inflammation, these radicals interact to generate peroxynitrite, a potent oxidant that causes severe cellular and tissue damage [46]. Similarly, PGE_2 induces vasodilation and enhances vascular permeability, which help guide immune cells to areas of tissue damage and support the repair process; however, it can also induce fever and pain and exacerbate inflammatory symptoms [47]. Selective COX-2 inhibitors are widely used to alleviate inflammation in clinical practice and suppress PGE_2 production by targeting COX-2 [48]. SSE not only lowered NO and PGE_2 production triggered by LPS but also downregulated iNOS and COX-2 mRNA levels, which encode the enzymes responsible for their production in macrophages, in a concentration-dependent manner. Pro-inflammatory cytokines play a central role in acute inflammatory processes by facilitating the differentiation, recruitment, and activation of immune cells and by mediating their interactions. Uncontrolled or prolonged cytokine production may lead to tissue injury, cytokine storms, persistent inflammation, and inflammation-related diseases. SSE significantly reduced LPS-stimulated secretion of IL-6, TNF-α, and IL-1β. Overall, these findings suggest that SSE mitigates inflammatory responses by limiting the excessive activation of inflammatory mediators within macrophages stimulated with LPS.

NF-κB represents a key group of transcription factors that govern diverse cellular responses to multiple external and internal signals, particularly within the immune system. It is divided into two subfamilies, the NF-κB proteins, including p50 (derived from p105) and p52 (derived from p100), and the Rel proteins, including RelA (also referred to as p65), RelB, and c-Rel. Dimerization between members of the NF-κB and Rel subfamilies is generally required for transcriptional activation, as p50 and p52 lack transactivation domains in contrast to Rel proteins [49]. NF-κB activity is strictly regulated by IκB proteins, particularly IκBα. IκBα directly binds to NF-κB p65/p50 heterodimers and suppresses their nuclear translocation, DNA binding, and transcriptional activation in resting cells. However, under stimulatory conditions, phosphorylation and subsequent degradation of IκBα result in the nuclear translocation of NF-κB [50]. Activation of the NF-κB signaling cascade ultimately induces the transcription of downstream genes. Furthermore, persistently elevated NF-κB activity in elderly individuals has been reported to drive a chronic and systemic inflammatory state known as inflammaging [51,52]. Recently, several studies have demonstrated that various natural product extracts and compounds can alleviate D-gal-induced tissue damage and delay aging by suppressing inflammatory responses through the NF-κB pathway. An extract of *Auricularia auricular* attenuated cognitive impairment and neuroinflammatory responses through the RAGE/MAPK/NF-κB signaling axis in D-gal-treated mice [53]. Wang et al. revealed that 6′-O-caffeoylarbutin, derived from *Vaccinium dunalianum*, improved inflammatory responses induced by D-gal by modulating the NF-κB and SIRT1 pathways in mouse brain as well as liver tissues [54]. Consistent with these findings, SSE significantly decreased NF-κB luciferase reporter activity and the phosphorylation levels of NF-κB in LPS-stimulated RAW 264.7 cells. Additionally, the mRNA expression levels of NF-κB and pro-inflammatory cytokines were significantly reduced in the hippocampus and cerebral cortex of SSE-administered mice. In particular, the changes in gene expression observed in the hippocampus may be associated with

the reduced phosphorylation levels of MAPKs (p38, JNK, and ERK1/2) in this region. MAPKs, including ERK1/2, JNK, and p38, are a family of kinases that mediate intracellular signaling in response to diverse extracellular and intracellular stimuli or stresses, thereby regulating cellular responses such as cell proliferation, differentiation, and inflammatory responses [55]. AP-1, which mainly consists of Jun, Fos, Maf, and ATF subunits, is a key dimeric transcription factor activated by MAPK signaling. The transcriptional activity of AP-1 is crucial for inflammatory responses, and its activation leads to the increased expression of pro-inflammatory genes [56]. A recent study reported that inhibition of AP-1 activity can partially reverse the senescence clock, and targeting AP-1 has been proposed as a promising strategy for modulating senescence [57]. SSE reduced AP-1 luciferase reporter activity and the phosphorylation levels of p38, JNK, and ERK1/2 in RAW 264.7 cells. In the mouse hippocampus, reduced phosphorylation of MAPKs may be associated with a potential decrease in AP-1 activity, as these kinases function upstream of AP-1. Additionally, the mRNA expression levels of TERT, p53, p21, and p16, recognized biomarkers of aging, were modulated in the SSE group. However, since no significant improvement in behavioral performance was observed in the passive avoidance test, the observed molecular changes cannot be conclusively linked to improvements in cognitive function. Therefore, future studies should include additional behavioral assessments, such as the Morris water maze, Y-maze, and novel object recognition tests, as well as extended treatment durations or different doses.

Other limitations of this study should be addressed as follows. First, a normal control group was not included in the in vivo experiments, and comparisons were focused on D-gal-injected groups with or without SSE administration. As a result, we could not directly assess baseline inflammatory and aging-related phenotypes under normal physiological conditions. However, administration of D-gal at a dose of 500 mg/kg/day is a well-established and widely used method to induce systemic inflammation and brain aging in mice [26,58,59], as demonstrated in numerous previous studies. Nevertheless, future studies including a normal control group will be necessary to further substantiate the baseline effects. Additionally, the small sample size and absence of a positive control group limit the interpretation of both molecular and behavioral findings. Second, as only a single dose of SSE was tested, the dose–response relationship could not be evaluated, making it difficult to determine the minimal or optimal effective dose. To address these limitations, future studies should include normal and positive control groups, multiple SSE dose groups, and larger sample sizes. In addition, detailed histopathological analyses and assessment of biomarkers such as ionized calcium-binding adapter molecule 1 and glial fibrillary acidic protein would provide further mechanistic and functional insights.

5. Conclusions

Findings from the present study indicate that SSE exerts anti-inflammatory effects in vitro and suggest its potential as a marine-derived candidate for further preclinical investigation in inflammation and age-related neuroinflammatory conditions. Further well-designed and comprehensive preclinical studies are required to confirm these findings and to clarify their translational relevance.

Author Contributions: Conceptualization, E.-J.P. and H.-J.L.; Methodology, S.-M.K., H.-S.P. and J.C.; Formal analysis, S.-M.K., E.-J.P. and H.-S.P.; Investigation, J.C.; Writing—original draft, S.-M.K. and E.-J.P.; Writing—review and editing, H.-J.L.; Visualization, H.-S.P.; Supervision, E.-J.P. and H.-J.L.; Project administration, H.-J.L.; Funding acquisition, H.-J.L. All authors have read and agreed to the published version of the manuscript.

Funding: This research was supported by Korea Institute of Marine Science & Technology Promotion (KIMST) funded by the Ministry of Oceans and Fisheries (RS-2023-00236592) and by the Gachon University research fund of 2025 (GCU-202503310001).

Institutional Review Board Statement: The animal study protocol was approved by the Institutional Animal Care and Use Committee of Gachon University (GU1-2024-IA0037).

Data Availability Statement: The original contributions presented in this study are included in the article. Further inquiries can be directed to the corresponding author.

Acknowledgments: We thank Ju-Hong Jeon (Seoul National University) for providing the 3 × κB-Luc reporter gene plasmid.

Conflicts of Interest: The authors declare no conflicts of interest.

Abbreviations

The following abbreviations are used in this manuscript:

AP-1	Activator protein 1
CCK-8	Cell Counting Kit-8
COX-2	Cyclooxygenase-2
D-gal	D-galactose
ERK	Extracellular signal-regulated kinase
IL-1β	Interleukin-1 beta
IL-6	Interleukin-6
iNOS	Inducible nitric oxide synthase
IκBα	NF-κB inhibitor alpha
JNK	c-Jun N-terminal kinase
KHFF	Korea Health Functional Food Institute
LPS	Lipopolysaccharide
MAPKs	Mitogen-activated protein kinases
MC	Model control
NF-κB	Nuclear factor kappa-B
NO	Nitric oxide
qRT-PCR	Quantitative reverse transcription polymerase chain reaction
SD	Standard deviation
SSE	*Sargassum siliquastrum* extract
TERT	Telomerase reverse transcriptase
TNF-α	Tumor necrosis factor-alpha

References

1. Medzhitov, R. Origin and physiological roles of inflammation. *Nature* **2008**, *454*, 428–435. [CrossRef] [PubMed]
2. Pahwa, R.; Goyal, A.; Jialal, I. *Chronic Inflammation*; StatPearls: Treasure Island, FL, USA, 2025.
3. Lin, T.; Liu, G.A.; Perez, E.; Rainer, R.D.; Febo, M.; Cruz-Almeida, Y.; Ebner, N.C. Systemic inflammation mediates age-related cognitive deficits. *Front. Aging Neurosci.* **2018**, *10*, 236. [CrossRef] [PubMed]
4. Lee, P.Y.; Li, Y.; Kumagai, Y.; Xu, Y.; Weinstein, J.S.; Kellner, E.S.; Nacionales, D.C.; Butfiloski, E.J.; van Rooijen, N.; Akira, S.; et al. Type I interferon modulates monocyte recruitment and maturation in chronic inflammation. *Am. J. Pathol.* **2009**, *175*, 2023–2033. [CrossRef] [PubMed]
5. Wang, M.; Wang, Y.; Wang, X.; Qiu, Y.; Li, C.; Li, H.; Li, H.; Yu, J. Lactoferrin ameliorates cognitive impairment in D-galactose-induced aging mice by regulating the PI3K/Akt/mTOR signaling pathway and the microbiome-gut-brain axis. *Int. J. Biol. Macromol.* **2025**, *309*, 143033. [CrossRef]
6. Zhang, X.; Wu, J.Z.; Lin, Z.X.; Yuan, Q.J.; Li, Y.C.; Liang, J.L.; Zhan, J.Y.X.; Xia, Y.L.; Su, Z.R.; Liu, Y.H. Ameliorative effect of supercritical fluid extract of *Chrysanthemum indicum* Linnén against D-galactose induced brain and liver injury in senescent mice via suppression of oxidative stress, inflammation and apoptosis. *J. Ethnopharmacol.* **2019**, *234*, 44–56. [CrossRef]
7. Brancewicz, J.; Wojcik, N.; Sarnowska, Z.; Robak, J.; Krol, M. The Multifaceted Role of Macrophages in Biology and Diseases. *Int. J. Mol. Sci.* **2025**, *26*, 2107. [CrossRef]

8. Hwang, J.-H.; Oh, Y.-S.; Lim, S.-B. Anti-inflammatory activities of some brown marine algae in LPS-stimulated RAW 264.7 cells. *Food Sci. Biotechnol.* **2014**, *23*, 865–871. [CrossRef]
9. Khumalo, G.P.; Nguyen, T.; Van Wyk, B.E.; Feng, Y.; Cock, I.E. Inhibition of pro-inflammatory cytokines by selected southern African medicinal plants in LPS-stimulated RAW 264.7 macrophages. *J. Ethnopharmacol.* **2024**, *319*, 117268. [CrossRef]
10. Woo, I.K.; Hyun, J.H.; Jang, H.J.; Lee, N.K.; Paik, H.D. Probiotic *Pediococcus acidilactici* Strains Exert Anti-inflammatory Effects by Regulating Intracellular Signaling Pathways in LPS-Induced RAW 264.7 Cells. *Probiotics Antimicrob. Proteins* **2024**, *17*, 3258–3269. [CrossRef]
11. Fang, Y.; Yang, L.; He, J. Plantanone C attenuates LPS-stimulated inflammation by inhibiting NF-kappaB/iNOS/COX-2/MAPKs/Akt pathways in RAW 264.7 macrophages. *Biomed. Pharmacother.* **2021**, *143*, 112104. [CrossRef]
12. Holdt, S.L.; Kraan, S. Bioactive compounds in seaweed: Functional food applications and legislation. *J. Appl. Phycol.* **2011**, *23*, 543–597. [CrossRef]
13. Belghit, I.; Rasinger, J.D.; Heesch, S.; Biancarosa, I.; Liland, N.; Torstensen, B.; Waagbø, R.; Lock, E.-J.; Bruckner, C.G. In-depth metabolic profiling of marine macroalgae confirms strong biochemical differences between brown, red and green algae. *Algal Res.* **2017**, *26*, 240–249. [CrossRef]
14. Guiry, M.D.; Guiry, G.M. AlgaeBase. World-wide Electronic Publication. National University of Ireland, Galway. Available online: https://www.algaebase.org (accessed on 18 August 2025).
15. Chopin, T.; Tacon, A.G. Importance of seaweeds and extractive species in global aquaculture production. *Rev. Fish. Sci. Aquac.* **2021**, *29*, 139–148. [CrossRef]
16. Seo, C.; Jeong, S.J.; Yun, H.J.; Lee, H.J.; Lee, J.W.; An, H.W.; Han, N.; Jung, W.K.; Lee, S.G. Nutraceutical potential of polyphenol-rich *Sargassum* species grown off the Korean coast: A review. *Food Sci. Biotechnol.* **2022**, *31*, 971–984. [CrossRef]
17. Woo, G.E.; Kim, M.J.; Ahn, D.H. In vitro and in vivo anti-inflammatory activities of ethanolic extract of *Sargassum confusum*. *Food Sci. Biotechnol.* **2024**, *33*, 181–190. [CrossRef]
18. Lee, Y.-H.; Kim, H.-R.; Yeo, M.-H.; Kim, S.C.; Hyun, H.-B.; Ham, Y.-M.; Jung, Y.-H.; Kim, H.-S.; Chang, K.-S. Anti-obesity potential of *Sargassum horneri* and *Ulva australis* extracts: Study in vitro and in vivo. *Appl. Sci.* **2023**, *13*, 8951. [CrossRef]
19. Natarajan, A.; Jayavelu, A.; Thangamani, R.; Prabakarakrishnan, R.; Choi, D.; Mohammed, A.; Khamis, H.; Kumar, B.S. In vivo evaluation of protective effect of *Sargassum fusiforme* on cisplatin induced hepato-renal toxicity. *Physiol. Mol. Plant Pathol.* **2022**, *117*, 101748. [CrossRef]
20. Jang, K.H.; Lee, B.H.; Choi, B.W.; Lee, H.S.; Shin, J. Chromenes from the brown alga *Sargassum siliquastrum*. *J. Nat. Prod.* **2005**, *68*, 716–723. [CrossRef]
21. Min, H.Y.; Kim, H.; Lee, H.J.; Yoon, N.Y.; Kim, Y.K.; Lee, H.Y. Ethanol Extract of *Sargassum siliquastrum* Inhibits Lipopolysaccharide-Induced Nitric Oxide Generation by Downregulating the Nuclear Factor-Kappa B Signaling Pathway. *Evid. Based Complement. Altern. Med.* **2022**, *2022*, 6160010. [CrossRef]
22. Singleton, V.L.; Orthofer, R.; Lamuela-Raventós, R.M. Analysis of total phenols and other oxidation substrates and antioxidants by means of folin-ciocalteu reagent. *Methods Enzymol.* **1999**, *299*, 152–178.
23. Chun, J.N.; Park, S.; Lee, S.; Kim, J.K.; Park, E.J.; Kang, M.; Kim, H.K.; Park, J.K.; So, I.; Jeon, J.H. Schisandrol B and schisandrin B inhibit TGFbeta1-mediated NF-kappaB activation via a Smad-independent mechanism. *Oncotarget* **2018**, *9*, 3121–3130. [CrossRef] [PubMed]
24. Vasanwala, F.H.; Kusam, S.; Toney, L.M.; Dent, A.L. Repression of AP-1 function: A mechanism for the regulation of Blimp-1 expression and B lymphocyte differentiation by the B cell lymphoma-6 protooncogene. *J. Immunol.* **2002**, *169*, 1922–1929. [CrossRef] [PubMed]
25. Kim, S.-M.; Park, E.-J.; Lee, H.-J. Nuciferine attenuates lipopolysaccharide-stimulated inflammatory responses by inhibiting p38 MAPK/ATF2 signaling pathways. *Inflammopharmacology* **2022**, *30*, 2373–2383. [CrossRef] [PubMed]
26. Chen, H.; Dong, L.; Chen, X.; Ding, C.; Hao, M.; Peng, X.; Zhang, Y.; Zhu, H.; Liu, W. Anti-aging effect of phlorizin on D-galactose-induced aging in mice through antioxidant and anti-inflammatory activity, prevention of apoptosis, and regulation of the gut microbiota. *Exp. Gerontol.* **2022**, *163*, 111769. [CrossRef]
27. Yu, Y.; Xue, B.; Liu, T.; Yue, X.; Liu, D.; Yu, X.; Xu, Y.; Zhao, X.; Li, X. Research on the Antiaging Activity of Licorice Water Extract in Aging Mice via Antioxidation, Neuronal Protection, Gut Microbiota Restoration, and PI3K/AKT/mTOR Modulation. *Mediat. Inflamm.* **2025**, *2025*, 8844859. [CrossRef]
28. Zhang, Y.; Ding, C.; Cai, Y.; Chen, X.; Zhao, Y.; Liu, X.; Zhang, J.; Sun, S.; Liu, W. Astilbin ameliorates oxidative stress and apoptosis in D-galactose-induced senescence by regulating the PI3K/Akt/m-TOR signaling pathway in the brains of mice. *Int. Immunopharmacol.* **2021**, *99*, 108035. [CrossRef]
29. Yamamoto, H.; Shimomura, N.; Oura, K.; Hasegawa, Y. Nacre Extract from Pearl Oyster Shell Prevents D-Galactose-Induced Brain and Skin Aging. *Mar. Biotechnol.* **2023**, *25*, 503–518. [CrossRef]

30. Zhang, Z.; He, S.; Cao, X.; Ye, Y.; Yang, L.; Wang, J.; Liu, H.; Sun, H. Potential prebiotic activities of soybean peptides Maillard reaction products on modulating gut microbiota to alleviate aging-related disorders in D-galactose-induced ICR mice. *J. Funct. Foods* **2020**, *65*, 103729. [CrossRef]
31. Lee, S.A.; Moon, S.M.; Choi, Y.H.; Han, S.H.; Park, B.R.; Choi, M.S.; Kim, J.S.; Kim, Y.H.; Kim, D.K.; Kim, C.S. Aqueous extract of *Codium fragile* suppressed inflammatory responses in lipopolysaccharide-stimulated RAW264.7 cells and carrageenan-induced rats. *Biomed. Pharmacother.* **2017**, *93*, 1055–1064. [CrossRef]
32. Premarathna, A.D.; Wijesekera, S.K.; Jayasooriya, A.P.; Waduge, R.N.; Wijesundara, R.R.M.K.K.; Tuvikene, R.; Harishchandra, D.L.; Ranahewa, T.H.; Perera, N.A.N.D.; Wijewardana, V.; et al. In vitro and in vivo evaluation of the wound healing properties and safety assessment of two seaweeds (*Sargassum ilicifolium* and *Ulva lactuca*). *Biochem. Biophys. Rep.* **2021**, *26*, 100986. [CrossRef]
33. Nurkolis, F.; Taslim, N.A.; Subali, D.; Kurniawan, R.; Hardinsyah, H.; Gunawan, W.B.; Kusuma, R.J.; Yusuf, V.M.; Pramono, A.; Kang, S.; et al. Dietary Supplementation of *Caulerpa racemosa* Ameliorates Cardiometabolic Syndrome via Regulation of PRMT-1/DDAH/ADMA Pathway and Gut Microbiome in Mice. *Nutrients* **2023**, *15*, 909. [CrossRef] [PubMed]
34. Reshma, B.S.; Aavula, T.; Narasimman, V.; Ramachandran, S.; Essa, M.M.; Qoronfleh, M.W. Antioxidant and Antiaging Properties of Agar Obtained from Brown Seaweed *Laminaria digitata* (Hudson) in D-Galactose-Induced Swiss Albino Mice. *Evid. Based Complement. Altern. Med.* **2022**, *2022*, 7736378. [CrossRef] [PubMed]
35. Su, Y.W.; Chiou, W.F.; Chao, S.H.; Lee, M.H.; Chen, C.C.; Tsai, Y.C. Ligustilide prevents LPS-induced iNOS expression in RAW 264.7 macrophages by preventing ROS production and down-regulating the MAPK, NF-kappaB and AP-1 signaling pathways. *Int. Immunopharmacol.* **2011**, *11*, 1166–1172. [CrossRef] [PubMed]
36. Li, J.J.; Zhu, Q.; Lu, Y.P.; Zhao, P.; Feng, Z.B.; Qian, Z.M.; Zhu, L. Ligustilide prevents cognitive impairment and attenuates neurotoxicity in D-galactose induced aging mice brain. *Brain Res.* **2015**, *1595*, 19–28. [CrossRef]
37. Jung, M.; Jang, K.H.; Kim, B.; Lee, B.H.; Choi, B.W.; Oh, K.B.; Shin, J. Meroditerpenoids from the brown alga *Sargassum siliquastrum*. *J. Nat. Prod.* **2008**, *71*, 1714–1719. [CrossRef]
38. Yoon, W.J.; Heo, S.J.; Han, S.C.; Lee, H.J.; Kang, G.J.; Kang, H.K.; Hyun, J.W.; Koh, Y.S.; Yoo, E.S. Anti-inflammatory effect of sargachromanol G isolated from *Sargassum siliquastrum* in RAW 264.7 cells. *Arch. Pharm. Res.* **2012**, *35*, 1421–1430. [CrossRef]
39. Heo, S.J.; Yoon, W.J.; Kim, K.N.; Oh, C.; Choi, Y.U.; Yoon, K.T.; Kang, D.H.; Qian, Z.J.; Choi, I.W.; Jung, W.K. Anti-inflammatory effect of fucoxanthin derivatives isolated from *Sargassum siliquastrum* in lipopolysaccharide-stimulated RAW 264.7 macrophage. *Food Chem. Toxicol.* **2012**, *50*, 3336–3342. [CrossRef]
40. Lee, J.H.; Ko, J.Y.; Samarakoon, K.; Oh, J.Y.; Heo, S.J.; Kim, C.Y.; Nah, J.W.; Jang, M.K.; Lee, J.S.; Jeon, Y.J. Preparative isolation of sargachromanol E from *Sargassum siliquastrum* by centrifugal partition chromatography and its anti-inflammatory activity. *Food Chem. Toxicol.* **2013**, *62*, 54–60. [CrossRef]
41. Qi, Y.; Wang, Z.; Zhang, J.; Tang, S.; Zhu, H.; Jiang, B.; Li, X.; Wang, J.; Sun, Z.; Zhao, M.; et al. Anti-Neuroinflammatory Meroterpenoids from a Chinese Collection of the Brown Alga *Sargassum siliquastrum*. *J. Nat. Prod.* **2023**, *86*, 1284–1293. [CrossRef]
42. Pan, J.; Liu, H.; Xu, J.; Xu, X.; Qi, Y.; Wang, C.; Wu, C.; Sun, Z.; Lv, Y.; Yan, P. Five new chromane meroditerpenoids from the brown alga *Sargassum siliquastrum* of China Sea. *Phytochem. Lett.* **2024**, *64*, 133–137. [CrossRef]
43. Pan, J.; Liu, H.; Xu, X.; Lv, F.; Qi, Y.; Wang, C.; Wu, C.; Sun, Z.; Xu, G.; Yan, P. Two New Chromane Meroditerpenoids with Anti-Neuroinflammatory Potential from a Chinese Collection of the Brown Alga *Sargassum siliquastrum*. *Nat. Product Commun.* **2025**, *20*, 1934578X251321614. [CrossRef]
44. Premarathna, A.D.; Tuvikene, R.; Somasiri, M.N.R.; De Silva, M.L.W.P.; Adhikari, R.; Ranahewa, T.H.; Wijesundara, R.R.M.K.K.; Wijesekera, S.K.; Dissanayake, I.P.G.H.U.; Wangchuk, P.; et al. A novel therapeutic effect of mannitol-rich extract from the brown seaweed *Sargassum ilicifolium* using in vitro and in vivo models. *BMC Complement. Med. Ther.* **2023**, *23*, 26. [PubMed]
45. Anokwah, D.; Kwatia, E.A.; Amponsah, I.K.; Jibira, Y.; Harley, B.K.; Ameyaw, E.O.; Obese, E.; Biney, R.P.; Mensah, A.Y. Evaluation of the anti-inflammatory and antioxidant potential of the stem bark extract and some constituents of *Aidia genipiflora* (DC.) dandy (rubiaceae). *Heliyon* **2022**, *8*, e10082. [CrossRef] [PubMed]
46. Coleman, J.W. Nitric oxide in immunity and inflammation. *Int. Immunopharmacol.* **2001**, *1*, 1397–1406. [CrossRef]
47. Gomez, I.; Foudi, N.; Longrois, D.; Norel, X. The role of prostaglandin E2 in human vascular inflammation. *Prostaglandins Leukot. Essent. Fat. Acids* **2013**, *89*, 55–63. [CrossRef]
48. Ju, Z.; Li, M.; Xu, J.; Howell, D.C.; Li, Z.; Chen, F.E. Recent development on COX-2 inhibitors as promising anti-inflammatory agents: The past 10 years. *Acta Pharm. Sin. B* **2022**, *12*, 2790–2807. [CrossRef]
49. Gilmore, T.D. Introduction to NF-kappaB: Players, pathways, perspectives. *Oncogene* **2006**, *25*, 6680–6684. [CrossRef]
50. Oeckinghaus, A.; Ghosh, S. The NF-kappaB family of transcription factors and its regulation. *Cold Spring Harb. Perspect. Biol.* **2009**, *1*, a000034. [CrossRef]
51. Kriete, A.; Mayo, K.L.; Yalamanchili, N.; Beggs, W.; Bender, P.; Kari, C.; Rodeck, U. Cell autonomous expression of inflammatory genes in biologically aged fibroblasts associated with elevated NF-kappaB activity. *Immun. Ageing* **2008**, *5*, 5. [CrossRef]

52. Chung, H.Y.; Kim, D.H.; Lee, E.K.; Chung, K.W.; Chung, S.; Lee, B.; Seo, A.Y.; Chung, J.H.; Jung, Y.S.; Im, E.; et al. Redefining Chronic Inflammation in Aging and Age-Related Diseases: Proposal of the Senoinflammation Concept. *Aging Dis.* **2019**, *10*, 367–382. [CrossRef]
53. Wang, J.; Zhang, T.; Liu, X.; Fan, H.; Wei, C. Aqueous extracts of se-enriched *Auricularia auricular* attenuates D-galactose-induced cognitive deficits, oxidative stress and neuroinflammation via suppressing RAGE/MAPK/NF-kappaB pathway. *Neurosci. Lett.* **2019**, *704*, 106–111. [CrossRef] [PubMed]
54. Wang, Y.; Wang, Y.; Zhao, T.; Zhou, W.; Khan, A.; Cao, J.; Liu, Y.; Wang, Z.; Cheng, G. 6′-O-caffeoylarbutin attenuates D-galactose-induced brain and liver damage in aging mice via regulating SIRT1/NF-kappaB pathway. *Phytomedicine* **2025**, *141*, 156710. [CrossRef]
55. Zhang, W.; Liu, H.T. MAPK signal pathways in the regulation of cell proliferation in mammalian cells. *Cell Res.* **2002**, *12*, 9–18. [CrossRef]
56. Janson, N.D.; Jehanathan, N.; Jung, S.; Priyathilaka, T.T.; Nam, B.H.; Kim, M.J.; Lee, J. Insight into the molecular function and transcriptional regulation of activator protein 1 (AP-1) components c-Jun/c-Fos ortholog in red lip mullet (*Liza haematocheila*). *Fish. Shellfish. Immunol.* **2019**, *93*, 597–611. [CrossRef]
57. Martinez-Zamudio, R.I.; Roux, P.F.; de Freitas, J.; Robinson, L.; Dore, G.; Sun, B.; Belenki, D.; Milanovic, M.; Herbig, U.; Schmitt, C.A.; et al. AP-1 imprints a reversible transcriptional programme of senescent cells. *Nat. Cell Biol.* **2020**, *22*, 842–855. [CrossRef]
58. Zhong, R.; Shen, L.; Fan, Y.; Luo, Q.; Hong, R.; Sun, X.; Zhou, X.; Wan, J. Anti-aging mechanism and effect of treatment with raw and wine-steamed *Polygonatum sibiricum* on D-galactose-induced aging in mice by inhibiting oxidative stress and modulating gut microbiota. *Front. Pharmacol.* **2024**, *15*, 1335786. [CrossRef]
59. Pan, J.; Chen, F.; Yu, L.; Hong, K.; Ye, Z.; Zhang, Q.; Zhang, C.; Zhao, J.; Zhai, Q.; Tian, F. *Ampelopsis grossedentata* tea polysaccharide alleviates D-galactose-induced aging in mice and regulates gut microbiota. *Food Biosci.* **2025**, *63*, 105635. [CrossRef]

Disclaimer/Publisher's Note: The statements, opinions and data contained in all publications are solely those of the individual author(s) and contributor(s) and not of MDPI and/or the editor(s). MDPI and/or the editor(s) disclaim responsibility for any injury to people or property resulting from any ideas, methods, instructions or products referred to in the content.